Narrow-Band Thermal Photonic Crystal Emitter for Mid-Infrared Applications [†]

Banafsheh Abasahl [1],*, Reyhaneh Jannesari [2] and Bernhard Jakoby [2]

[1] Carinthian Tech Research AG, Europastrasse 12, 9524 Villach, Austria

[2] Institute for Microelectronics and Microsensors, Johannes Kepler University, 4040 Linz, Austria; reyhaneh.jannesari@jku.at (R.J.); bernhard.jakoby@jku.at (B.J.)

* Correspondence: banafsheh.abasahl@gmail.com; Tel.: +43-424256-300-264

† Presented at the Eurosensors 2018 Conference, Graz, Austria, 9–12 September 2018.

Abstract: Mid-infrared (MIR) on-chip sensing on Si has been a progressive topic of research in the recent years due to excitation of vibrational and rotational bands specific to materials in this range and their immunity against visible light and electromagnetic interferences. For on-chip applications, integration of all the optical components including the MIR source is crucial. In this work, we introduce a slab photonic crystal (PhC) thermal source where the birthplace and the filtering of the photons occur in the same region. Due to the forbidden frequency bands and high density of states in the band edge, it provides electric efficiency and filtering performance.

Keywords: photonic crystals; MIR thermal emitters; bandgap engineering; optical filters

1. Introduction

Silicon photonics technology, where the optical circuits are realized in CMOS technology and mainly in the telecommunication spectra, has opened up a new venue in the past two decades for achieving on-chip optical devices. Advances in this domain at the telecommunication wavelengths have laid the groundwork of utilizing this technology in other spectral ranges, such as visible and MIR. For sensing applications, the MIR domain is of a great interest, since the absorption peak due to photon-phonon coupling of the many simple molecules falls within this regime [1]. It has been shown that high performance though expensive and bulky spectroscopy can be reached with a sensitivity of down to part per trillion [2,3]. However, reaching such a performance in fully integrated system on chip device is far from trivial [4,5]. One of the challenges that had to be addressed in this domain is to provide on-chip and low cost optical sources. It has been shown that group III-V compounds interband cascade and quantum cascade devices can provide MIR sources [6–10]. However, these compounds are not compatible to be efficiently grown onto the silicon platform which make the device manufacturing complicated and expensive. In this work, a thermal source in a photonic crystal lattice filter is studied for an on-chip gas sensing application based on Si photonics [11,12]. Such a system is fully compatible with the routines of CMOS fabrication plants and can result in functional chips with a reduced price. Our approach is based on controlled thermal generation of photons in the wavelength of interest in a series of slab PhCs with different lattice parameters. The forbidden bandgaps of the PhCs are designed and arranged so that only photons at a narrow-band window of interest are allowed to be emitted or leave the emitter to the rest of the on-chip devices. In this work, optical analysis were performed with finite element time domain (FDTD) method using the commercially available package of R-Soft and the thermal property of the system was analyzed using COMSOL Multiphysics.

2. System under Study

A system of PhC holes on a Si slab has been developed to serve as a source for a Si slab waveguide. This system will be later adapted to an evanescent-field silicon waveguide platform for sensing CO_2 gas; and therefore, it is designed to emit at a wavelength of 4.26 μm [11].

A PhC lattice with a band gap region can be considered as a band-stop filter. By combining two PhC filters with different band stops, a narrow passage within a certain frequency window can be designed. In this work, our working window is $0.2 < \omega a/2\pi c < 0.5$, where c is the speed of light in the free space, ω is the radial frequency and a is the lattice constant. Figure 1a shows the arrangement of the proposed thermal emitter. The system comprises four main regions based on PhCs with various dimensions: filters 1 and 2, a mirror and a matching interface. The choice for the dimensions of the two filters and the mirror section is based on a gap map of Figure 1c. In this diagram, the first transverse magnetic (TM) gap of a hexagonally-arranged photonic crystal lattice is extracted with respect to the variation of the hole radius to the lattice constant r/a.

(a)

(b)

(c)

(d)
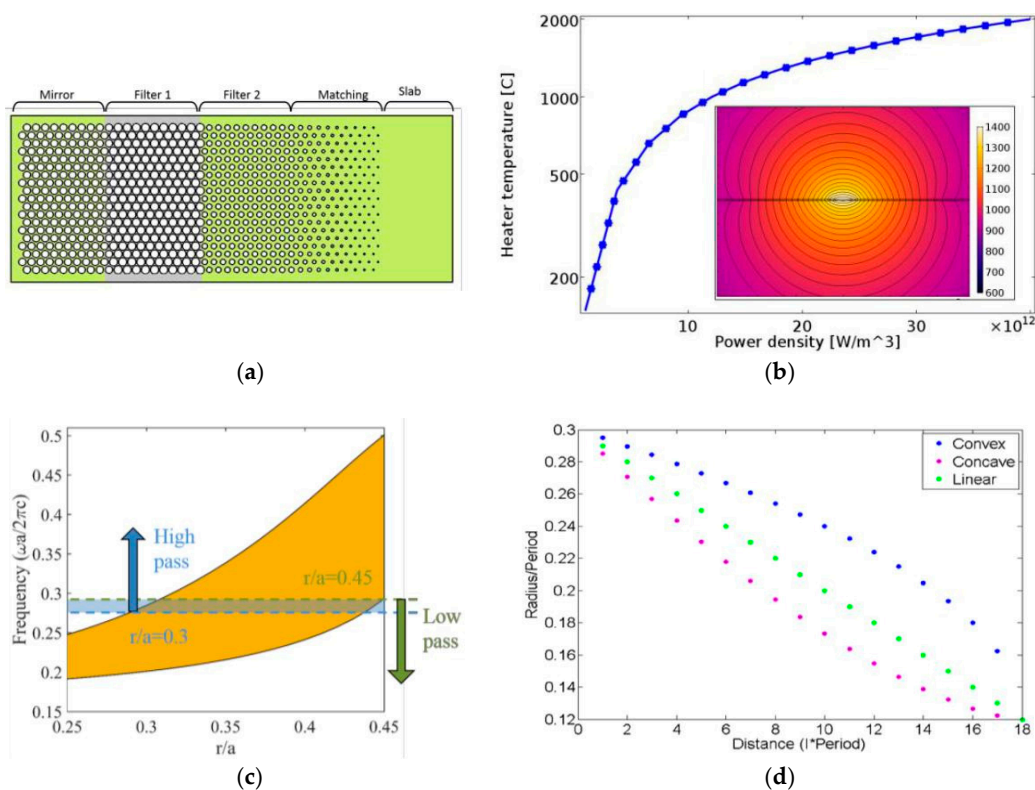
Figure 1. (**a**) Schematic representation of the 2D PhC thermal emitter, the green and gray shades corresponding, respectively to undoped and doped Poly-Si. (**b**) Temperature of the doped region as a function of the input power calculated considering the heat equation, photo-emissivity and laminar flow of air, inset: the temperature map at the cross section of the structure, color bar: the corresponding temperature. (**c**) Gap map of a PhC of holes in doped-Si as a function of the normalized hole radius for a periodicity of a = 1250 [nm]. Arrows up and down show the pass frequency range of the Filter 2 and 1 respectively. (**d**) The radii of the holes in the adiabatic region as a function of their distance from the beginning of the region.

Filter 1, with r/a = 0.45, is considered to be doped Poly-Si with a concentration of 1×10^{20} cm^{-3} to serve both as the emitter and filter. In other words, the birth place of the thermally generated photons is a lattice which suppresses the emission of those photons with an energy lying within their band gap. Based on the gap map of Figure 1c, filter 1 acts as a low pass filter in our working window, and suppresses photon of a normalized energy higher than $\omega a/2\pi c$ = 0.295. Being conductive, filter 1 carries an electric current in order to heat the region up to relatively high temperatures. The high temperature of this region is shown in Figure 1b as a function of input

electric power density, induces Planck's black body radiation. Since the generation of these photons occurs in the filters 1, no photon with energy within the corresponding bandgap has the chance of propagating in the crystal. As a result, the emission from such structure is already selectively filtered around the working frequency band. The second filter, with $r/a = 0.3$, acts as a high pass filter within our working area and blocks the propagation of the photons with a normalized energy lower than $\omega a/2\pi c = 0.27$. The mirror region, with $r/a = 0.35$, has a band gap covering our frequency of interest, and therefore, it reflects back the photons of the energy $0.286 < \omega a/2\pi c < 0.296$ travelling in (-x) direction into the guiding area. Finally, the matching section provides an adiabatic change of the PhC mode to the slab mode reducing unwanted reflection due to momentum mismatch. The center of the holes of the adiabatic region has been considered to follow the position of a lattice with a constant of the one for filter 2, while the radii of its hole would decrease following the below formula:

$$r(x) = r_0 + (r_0 - rf)[(1 - xL)\beta - 1], \tag{1}$$

where L is the length of the matching part, r_0 is the radius of holes in filter 2, rf is the smallest radius of the holes and $\beta = 0.5$, 1, or 1.5 is a damping coefficient which determines whether the transition is concave, linear or convex, respectively. Figure 1d shows three graphs for which the transition has changed from concave to linear and convex. The damping rate α for which the intensity drops exponentially throughout the propagation with a factor of $e^{-\alpha L}$, for the three different kinds of matching with similar length L is $a = 1.2 \times 10^{-4}$ μm^{-1}, 8.4×10^{-4} μm^{-1} and 7.7×10^{-4} μm^{-1}, respectively. At the free space wavelength of 4.26 μm, according to this calculation, the concave matching provide less in-plane loss for this structure, which suggests that a concave transition is a more suitable choice for our design.

3. Results and Discussion

To model the emittance of PhC emitter we use Kirchoff's law, stating that emittance and absorptance are equivalent [13]. The reflection and/or transmission spectra of each individual parts of the system are shown in Figure 2a–c. For the simulation, a TM mode is first excited in a slab and its reflection and transmission were recorded. The structures were terminated with a perfect matching layer (PML) in order to prevent unwanted reflections. Figure 2a shows the reflection from the filter1 and 2. The narrow wavelength range with low reflection for both filters corresponds to the emittance wavelength range of the emitter. Figure 2b shows a close to 100% reflection of the mirror throughout our working wavelength window. Figure 2c shows that almost 80% intensity of the light produced in the emitter passes through matching layer and is converted to slab mode.

The absorption and energy density spectra of the whole system for the case of filter 1 being doped and undoped, respectively, are shown in Figure 2d, based on which the system provides well-defined absorption at around the wavelength of our interest ($\lambda_0 = 4.26$ [μm]), and suppresses the other wavelengths around this region. Small mismatched between energy density and absorption spectra in Figure 2d is because of the difference in the refractive index of the doped and undoped silicon. Since the ensemble emissivity of such system is equal to its absorbance, the result of Figure 2d also represents its emitting performance.
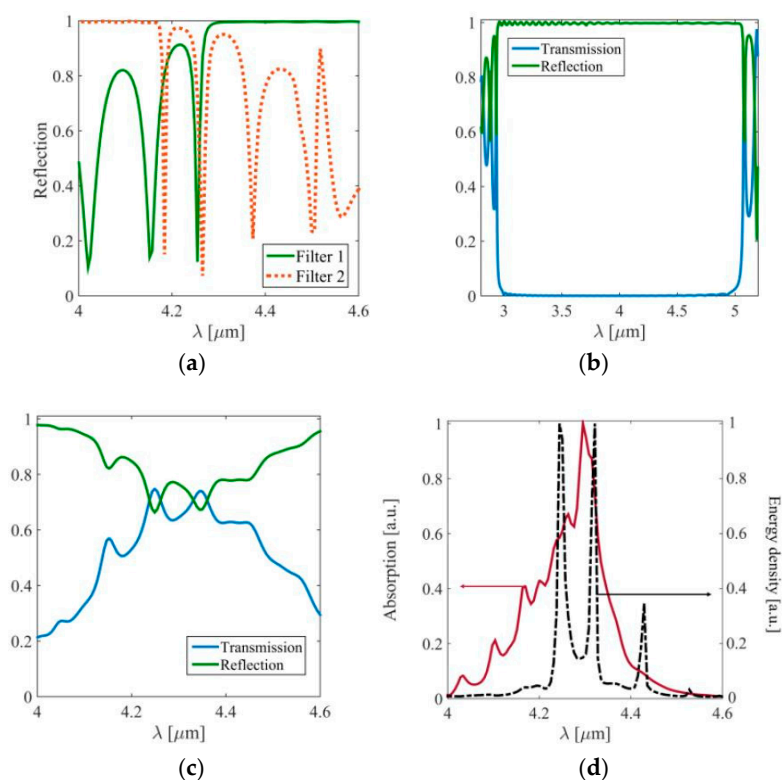
Figure 2. Optical response of the individual sections of the structure: (**a**) Filters 1 and 2; (**b**) Mirror; (**c**) Matching section; (**d**) Response of the whole structure for an excitation of the fundamental slab mode in the slab region; Red thick line corresponds to the absorption of the system when filter 1 is undoped and black dashed line shows the energy density when all components are undoped.

4. Conclusions

In this work, we presented the design of an on-chip Si-based thermal emitter based on PhC band engineering. This emitter tends to be used as a mid-infrared source for CO_2 gas sensing. The system is based on filtering out the broadband Planck's black body radiation so that the sensing path only carries the photons with high absorption probability for CO_2 and it prevent interaction of light with other molecules in other wavelengths. The implementation of the proposed structure can be easily adapted to the standard MEMS technology and the dimensions can be updated based on the frequency range of interest.

Author Contributions: B.A. and, R.J. developed the concept, performed the computations and wrote the manuscript; B.J. supervised the project and contributed in writing the manuscript.

Conflicts of Interest: The authors declare no conflict of interest.

References

1. Sieger, M.; Mizaikoff, B. Toward On-Chip Mid-Infrared Sensors. *Anal. Chem.* **2016**, *88*, 5562–5573. doi:10.1021/acs.analchem.5b04143.
2. Tomberg, T.; Vainio, M.; Hieta, T.; Halonen, L. Sub-parts-per-trillion level sensitivity in trace gas detection by cantilever-enhanced photo-acoustic spectroscopy. *Sci. Rep.* **2018**, *8*, 1848. doi:10.1038/s41598-018-20087-9.
3. Peltola, J.; Hieta, T.; Vainio, M. Parts-per-trillion-level detection of nitrogen dioxide by cantilever-enhanced photo-acoustic spectroscopy. *Opt. Lett.* **2015**, *40*, 2933–2936. doi:10.1364/OL.40.002933.

4. Singh, V.; Lin, P.T.; Patel, N.; Lin, H.; Li, L.; Zou, Y.; Deng, F.; Ni, C.; Hu, J.; Giammarco, J.; et al. Mid-infrared materials and devices on a Si platform for optical sensing. *Sci*. *Technol*. *Adv*. *Mater*. **2014**, *15*, 014603. doi:10.1088/1468-6996/15/1/014603.

5. Hu, T.; Dong, B.; Luo, X.; Liow, T.Y.; Song, J.; Lee, C.; Lo, G.Q. Silicon photonic platforms for mid-infrared applications [Invited]. *Photonics Res*. **2017**, *5*, 417–430. doi:10.1364/PRJ.5.000417.

6. Wang, R.; Vasiliev, A.; Muneeb, M.; Malik, A.; Sprengel, S.; Boehm, G.; Amann, M.C.; Šimonytė, I.; Vizbaras, A.; Vizbaras, K.; et al. III–V-on-Silicon Photonic Integrated Circuits for Spectroscopic Sensing in the 2–4 μm Wavelength Range. *Sensors* **2017**, *17*, doi:10.3390/s17081788.

7. Razeghi, M.; Lu, Q.Y.; Bandyopadhyay, N.; Zhou, W.; Heydari, D.; Bai, Y.; Slivken, S. Quantum cascade lasers: From tool to product. *Opt*. *Express* **2015**, *23*, 8462–8475. doi:10.1364/OE.23.008462.

8. Mermelstein, C.; Simanowski, S.; Mayer, M.; Kiefer, R.; Schmitz, J.; Walther, M.; Wagner, J. Room-temperature low-threshold low-loss continuous-wave operation of 2.26 μm GaInAsSb/AlGaAsSb quantum-well laser diodes. *Appl*. *Phys*. *Lett*. **2000**, *77*, 1581–1583. doi:10.1063/1.1308537.

9. Yao, Y.; Hoffman, A.J.; Gmachl, C.F. Mid-infrared quantum cascade lasers. *Nat*. *Photonics* **2012**, *6*, 432.

10. Belahsene, S.; Naehle, L.; Fischer, M.; Koeth, J.; Boissier, G.; Grech, P.; Narcy, G.; Vicet, A.; Rouillard, Y. Laser Diodes for Gas Sensing Emitting at 3.06 <formula formulatype="inline"><tex Notation="TeX">mu</tex></formula>m at Room Temperature. *IEEE Photonics Technol*. *Lett*. **2010**, *22*, 1084–1086. doi:10.1109/LPT.2010.2049989.

11. Ranacher, C.; Consani, C.; Hedenig, U.; Grille, T.; Lavchiev, V.; Jakoby, B. A photonic silicon waveguide gas sensor using evanescent-wave absorption. *IEEE Sens.* **2016**, doi:10.1109/ICSENS.2016.7808688.

12. Jannesari, R.; Ranacher, C.; Consani, C.; Grille, T.; Jakoby, B. Sensitivity optimization of a photonic crystal ring resonator for gas sensing applications. *Sensors Actuators A Physical* **2017**, doi:10.1016/j.sna.2017.08.017.

13. Luo, C.; Narayanaswamy, A.; Chen, G.; Joannopoulos, J.D. Thermal Radiation from Photonic Crystals: A Direct Calculation. *Phys*. *Rev*. *Lett*. **2004**, *93*, 213905. doi:10.1103/PhysRevLett.93.213905.